Tree Physiology 36, 1485–1497
doi:10.1093/treephys/tpw072

Research paper

First insights into the functional role of vasicentric tracheids and parenchyma in eucalyptus species with solitary vessels: do they contribute to xylem efficiency or safety?

Antonio José Barotto[1,2,6], María Elena Fernandez[2,3], Javier Gyenge[2,3], Ariel Meyra[2,4], Alejandro Martinez-Meier[5] and Silvia Monteoliva[1,2]

[1]Facultad de Ciencias Agrarias y Forestales, Universidad Nacional de La Plata, Diagonal 113 469, (1900) La Plata, Argentina; [2]Consejo Nacional de Investigaciones Científicas y Técnicas (CONICET), Av. Rivadavia 1917, (C1033AAJ) CABA, Argentina; [3]INTA, EEA Balcarce-Oficina Tandil, Gral. Martín Rodríguez 370, (7000) Tandil, Argentina; [4]Instituto de Física de Líquidos y Sistemas Biológicos (IFLYSIB-UNLP-CONICET), Calle 59 789, (1900) La Plata, Argentina; [5]INTA, EEA Bariloche, Modesta Victoria 4450, (8400) Bariloche, Argentina; [6]Corresponding author (jbarotto@conicet.gov.ar)

Received February 11, 2016; accepted July 5, 2016; published online September 10, 2016; handling Editor Guillermo Goldstein

The relationship between hydraulic specific conductivity (k_s) and vulnerability to cavitation (VC) with size and number of vessels has been studied in many angiosperms. However, few of the studies link other cell types (vasicentric tracheids (VT), fibre–tracheids, parenchyma) with these hydraulic functions. *Eucalyptus* is one of the most important genera in forestry worldwide. It exhibits a complex wood anatomy, with solitary vessels surrounded by VT and parenchyma, which could serve as a good model to investigate the functional role of the different cell types in xylem functioning. Wood anatomy (several traits of vessels, VT, fibres and parenchyma) in conjunction with maximum k_s and VC was studied in adult trees of commercial species with medium-to-high wood density (*Eucalyptus globulus* Labill., *Eucalyptus viminalis* Labill. and *Eucalyptus camaldulensis* Dehnh.). Traits of cells accompanying vessels presented correlations with functional variables suggesting that they contribute to both increasing connectivity between adjacent vessels—and, therefore, to xylem conduction efficiency—and decreasing the probability of embolism propagation into the tissue, i.e., xylem safety. All three species presented moderate-to-high resistance to cavitation (mean P_{50} values = −2.4 to −4.2 MPa) with no general trade-off between efficiency and safety at the interspecific level. The results in these species do not support some well-established hypotheses of the functional meaning of wood anatomy.

Keywords: *Eucalyptus camaldulensis*, *Eucalyptus globulus*, *Eucalyptus viminalis*, imperforate tracheary elements, vulnerability to cavitation, xylem connectivity, xylem hydraulic conductivity.

Introduction

The wood of angiosperm species is anatomically more complex than that of gymnosperms, presenting an axial system composed of vessels for water transport, a dense matrix of fibres for support and variable amounts of parenchyma for carbohydrate storage. There are other cell types with intermediate anatomy and function between vessels and fibres, such as tracheids and fibre–tracheids (Carlquist 1985). The anatomical complexity of wood in these species contributes to the coordinated water transport process, which depends directly on vessel characteristics and indirectly on the set of accompanying cells.

Hydraulic conduction function of imperforate tracheary elements (such as vasicentric tracheids (VTs) and fibre–tracheids) has been poorly studied (Carlquist 1985, 2012). Recently, Sano et al. (2011) have demonstrated that the conductive function of these elements depends fundamentally on the pit pair structure, size and density that connect them with the vessels. According to some authors, the function of tracheids in angiosperm species with solitary vessels, as in the case of *Eucalyptus* spp. or some *Quercus* spp., is essential to vessel communication (Carlquist 2012), thereby increasing xylem connectivity (Loepfe et al. 2007, Martínez-Vilalta et al. 2012). Also, it has been

proposed (Carlquist 1985) that VTs could constitute a subsidiary water conduction system when the main one—formed by vessels—is cavitated, allowing basal water flow to reach some degree of gas exchange under water deficit conditions. This theory suggests that VTs are less vulnerable to cavitation than vessels, and that there is a certain degree of isolation between them, which prevents air entry from a cavitated vessel. This would imply that wood with a greater proportion of VTs will be more resistant to xylem cavitation than that with a lower proportion of this cell type, even when both show similar vessel and VT characteristics. However, VTs could act as water reservoirs, thereby increasing tissue capacitance (Scholz et al. 2007, Ziemińska et al. 2013, Oliva Carrasco et al. 2015, Pfautsch et al. 2015). In this case, a higher vulnerability to cavitation (VC) of VTs—compared with vessels—could facilitate the release of tensions within the xylem. To our knowledge, no studies have elucidated this alternative role of VTs (conduction, capacitance, cavitation resistance) in species with solitary vessels, thus requiring studies that combine both anatomical and ecophysiological approaches.

Hydraulic specific conductivity of a wood portion (k_s) is directly related to xylem porosity (Tyree and Ewers 1991) and therefore, in angiosperms, vessel size and number. It is functionally related to photosynthetic carbon assimilation rates (Hubbard et al. 2001, Santiago et al. 2004), and plant growth (e.g., Brodribb et al. 2005, Kondoh et al. 2006) and survival. Several studies have shown the strong adaptive value of resistance to k_s losses (VC), with different species showing a decrease in VC with increasing aridity (Pockman and Sperry 2000, Maherali et al. 2004). However, VC seems to be a key trait associated with drought resistance in species having a tolerance strategy (sensu Levitt 1980), while other species may resist water stress by means of a more avoidant strategy (Levitt 1980). In these species, which may be quite vulnerable to cavitation, dehydration and high xylem tension are prevented or delayed through a high overall hydraulic conductance (favoured by high k_s), high tissue capacitance and a strong stomatal control of minimum leaf water potential (Meinzer and McCulloh 2013).

The relationship between k_s and VC with size and number of vessels has been studied in several angiosperm species (Tyree and Zimmermann 2002, Wheeler et al. 2005, Loepfe et al. 2007, Cai and Tyree 2010). Results indicate that the larger the vessel diameter, the higher the conductivity and VC (although there is no direct causal relationship between vessel diameter and VC). However, there are few studies linking other cell types, like VTs, fibre–tracheids, rays and axial parenchyma, to k_s and VC, with no available information at all for the *Eucalyptus* genus, which is the object of this study.

Hacke et al. (2009) demonstrated that—for woody species in the Californian desert (USA) whose anatomy have tracheids (vasicentric and vascular)—certain differences in cavitation resistance could not be explained by pit area per vessel (pit area hypothesis). Therefore, when discussing the results, they incorporated the idea that the pit area between vessels and tracheids should be included to explain the patterns found, since it increases system connectivity. Moreover, a recent study in *Hippophae rhamnoides* (Cai et al. 2014) suggests the importance of fibre–tracheids surrounding vessels as responsible for the existence of 'recalcitrant VC curves'. These curves are made up of two phases, one of which has greater vulnerability that could be due to cavitation of the vessels connected directly with other vessels; and a second phase, more resistant, corresponding to vessels interconnected by fibre–tracheids 'bridges'. These cells could contribute to the interconnection among vessels necessary to maintain k_s, and yet, decrease the likelihood of embolism propagation.

Eucalyptus is one of the most important genera in forestry, with over 20 million hectares planted worldwide (Iglesias-Trabado and Wilstermann 2009). It is a very diverse genus with ~700 species occupying a wide variety of ecological niches. The wood of this genus exhibits particular characteristics: diffuse porosity; mostly solitary vessels; diagonal vessel arrangement; simple perforation plates; alternate and vestured intervessel pits with elliptical included aperture; VT; fibres with circular or angular contour differentiated into two types, one with simple pits and other with bordered pits (fibre–tracheids); and vasicentric-paratracheal and/or diffuse-apotracheal axial parenchyma (Dadswell 1972). This complex anatomy may be partly a reflection of the high adaptive radiation of the genus.

This study aims to relate wood anatomy of branches with hydraulic conductivity and VC in three *Eucalyptus* species. The intention is to contribute to the knowledge of the functional value of wood in this genus (with complex wood anatomy) because it provides a model system for studying the contribution of the different cell types in the xylem hydraulic functioning. For this purpose, we selected three *Eucalyptus* species characterized by having medium (*Eucalyptus globulus* and *Eucalyptus viminalis*) and high (*Eucalyptus camaldulensis*) wood density (Insidewood 2004-onwards). Our hypotheses-predictions were: (a) if VTs (and other cells surrounding vessels: axial parenchyma and fibre–tracheids) mainly contribute to decrease VC, then there would be differences among species in VT proportion according to their VC (i.e., more VT in species or genotypes with high cavitation resistance); alternatively, (b) if VT contribute mostly to increase xylem connectivity, acting as hydraulic bridges, there would be differences among species in the amount of VT (and other cells surrounding vessels) which would help to explain differences in maximum hydraulic specific conductivity ($k_{s\ max}$), besides those arising from changes in vessel diameter; (c) vessel average size and diameter distribution in these species with solitary vessels would result in weak or no trade-off between k_s and VC across species or genotypes, since this trade-off arises from vessel-to-vessel connection in species with grouped vessels; and (d) no relationship is expected between parameters describing VC and vessel wall reinforcement, in contrast to that postulated by Hacke et al. (2001) as a general rule for conifers

and angiosperms, since their theory is based on the fact that a conducting vessel (i.e., under tension) in direct connection with an embolized vessel would collapse due to impairment of forces at the two sides of the cell wall, therefore requiring a particular minimum wall width for any lumen diameter. However, we still expect (e) a relationship between wood density and VC in *Eucalyptus* species, with *E. camaldulensis* being more resistant than *E. viminalis*, and the latter slightly more resistant than *E. globulus*. This relationship between wood density and VC would be mediated by the need for a fibre-matrix surrounding vessels with thick cell walls, to provide increased mechanical support as water is transported through xylem under high tension in cavitation-resistant species (Jacobsen et al. 2005).

Materials and methods

Plant material

The study was carried out using plant material from a total of 15 adult specimens (15–25 m tall) of *E. camaldulensis* ($n = 5$), *E. viminalis* ($n = 4$) and *E. globulus* ($n = 6$) growing in the same place (Tandil, Buenos Aires province, Argentina; 37°20′36″ S, 59°08′04″ W) in non-commercial plantations. Branches were collected from the basal portion of the crown (between 1.5 and 3 m from the ground), ensuring that they have similar dimensions (>1.5 m length). Before the final sampling reported here, maximum vessel length was determined by the air injection method (Greenidge 1952) in each species, which was found to vary between 50 and 72 cm.

Vulnerability to cavitation curves

Preliminary VC curves were performed with the air injection method in several branches of different lengths (see Figure S1 available as Supplementary Data at *Tree Physiology* Online with examples of these preliminary measurements). Those made with segments ~30 cm produced sigmoid curves (s-shaped) while segments of ~20 cm gave r-shaped curves. While it is known that some long vessels are cut, for operational reasons trying to avoid branch ramifications, and because the curves showed reasonable patterns, we decided to work with 30-cm long segments of 4–6 mm in diameter. Branches ($n = 4$–6, depending on the species) were collected during spring, in the early morning (between 8:00 and 9:00 AM) and placed in black polyethylene bags that were sprayed with water to achieve a fully saturated environment in order to prevent dehydration.

The curves were developed using a Scholander pressure chamber (model 10, BioControl, Buenos Aires, Argentina) with a cavitation chamber attached to it. After trying different pressurization and stabilization times (preliminary measurements in other branches), the final protocol followed was

(i) perfusion during 5 min at 1 Bar pressure to remove any initial embolism;
(ii) maximum k_s measurement ($k_{s\ max}$) with the pipette method (Sperry et al. 1988);
(iii) constant pressure applied within the cavitation chamber for 2 min (from 0.5 to 7.8 MPa);
(iv) stabilization for at least 5 min (or until no bubbles came out from the branch segment) during which water flowed through the branch; and
(v) k_s measurement.

Steps (i) and (ii) were performed only at the beginning of each curve, whereas Steps (iii)–(v) were repeated for each point of every curve.

The percentage loss of hydraulic conductivity (PLC) was estimated from the k_s losses for every imposed pressure level in relation to the maximum k_s ($k_{s\ max}$) of each branch. Then, first, the sigmoid function described by Pammenter and Vander Willigen (1998) was fitted, but due to its lack of fit in the lower pressure levels for *E. globulus*, the use the cumulative density function (CDF) of Weibull distribution was preferred. The Weibull model has been proposed as the most useful for curves with different forms, more and less sigmoid (Sperry et al. 2012, cited in Cai et al. 2014)

$$\frac{\mathrm{PLC}}{100} = 1 - \exp\left[-\left(\frac{T}{b}\right)^{c}\right],$$

where T is the tension (applied in the cavitation chamber), b is the Weibull scale parameter and c is the Weibull shape parameter. Usual parameters like P_{50}, P_{12} and P_{88}, that is, pressure inducing 50, 12 and 88% losses of hydraulic conductivity, and the slope between P_{12} and P_{88} of each VC curve (which denotes how fast conductivity is lost) were estimated from this model. P_{12} corresponds to air entry point (Sparks and Black 1999), and P_{88} is considered the point beyond which xylem becomes completely non-conductive (Domec and Gartner 2001).

Anatomical variables

Once VC curves were done, branches were adequately conditioned to obtain histological sections for anatomical measurements ($n = 4$–6 branches per species). Cross sections (20–25 μm thick) of the entire transversal branch section were obtained using a sliding microtome. Histological sections were not stained (see below) and were mounted in water. In addition, macerations were prepared according to Franklin (1945) for counting fibres and tracheids and measuring their lengths. One centimetre length segments were cut from each branch and soaked in a 1:1 glacial acetic acid:hydrogen peroxide solution. Cross-sectional and maceration images were captured with a digital camera (Infinity1-2CB, Lumenera Corporation, Ottawa, Canada) mounted on a research microscope (CX31, Olympus, Tokyo, Japan), using a magnification of ×4 (20–25 images to capture the entire branch transversal section) and ×20 (20 images to cover two complete radial sections from pith to bark). Captured images were analysed using image analysis software (ImagePro Plus 6.0, Media Cybernetics, Carlsbad, CA, USA).

Figure 1. Methodology for determining halo area around vessels. Unstained transverse sections (×20) of *E. globulus* showing solitary vessels surrounded by 'halos', composed of VTs and axial parenchyma (left panel). The halo area was manually set (central panel) and then the vessel area was substracted (right panel).

The following variables were measured in transverse sections (how they were measured is explained below): vessel diameter (μm), vessel number (mm^{-2}) and halo (this term is used to refer to all companion cells surrounding a solitary vessel, and it is composed of VTs and axial parenchyma). In transverse sections, it is not possible to differentiate tracheids from axial parenchyma; this is achieved by observation in longitudinal sections or in macerations. Lack of staining in cuts made it possible to highlight the halo (adjusting gamma levels on images to increase contrast) for better quantification (Figure 1). The halo area measurement was made on digital images of transverse sections using a magnification of ×20) area of companion cells surrounding each vessel (μm^2), halo area/vessel area, conduit wall reinforcement $(t/b)^2$, intervessel bridges (μm and cell number), vessel pit diameter (μm), VT pit diameter (μm), fibre wall thickness (μm), fibre lumen diameter (μm), fibre diameter (μm), rays ($n° mm^{-1}$) and vessel-ray contact area (%). In macerations, the following measurements were taken: fibre (%), fibre–tracheid (%), VT (%), axial parenchyma (%), fibre length (μm), VT length (μm) and vessel element length (μm). Wood density at 15% moisture content ($g\ cm^{-3}$) was determined.

The image processing software was used to mark the halo perimeter manually and to calculate its area automatically (Figure 1). We proceeded in this way with each individual vessel in all images (20 images per sample).

Vessel diameter and number were measured (digital images at ×20 magnification in transverse section; 20 images per sample) by automatically counting bright areas between 10 and 100 μm in diameter (count/size, automatic bright objects, ImagePro Plus 6.0, Media Cybernetics). Vessel percentage in different diameter size classes was fitted with Weibull probability density function (PDF):

$$\mathrm{PDFV}(x;\, b,\, c) \;=\; \frac{c}{b}\left(\frac{x}{b}\right)^{(c-1)} \exp\left[-\left(\frac{x}{b}\right)\right]^{c},$$

where b and c are fitting constants (equivalent to those of Weibull CDF) and x is the bin diameter increment defined as $x = dc/dw$, where dw is the width of vessel diameter size class (10 μm in our case) and dc is the diameter at the centre of the vessel diameter size class. Parameters b and c describe the amplitude and shape (more or less symmetrical) of vessel distribution, respectively, and were used for principal component analyses (PCA) and correlations analyses with the other anatomical and functional variables.

Pits from vessels and tracheids were measured manually in macerations at ×40 magnification. The longest axis of pit chambers ($n = 60$) in 20 cells per sample was determined. Intervessel bridges were manually measured in six to eight adjacent vessels per image (×20 magnification in transverse section; 20 images per sample). Distance between vessels (in μm) was determined in radial and tangential directions, and the number of cells within that distance was counted. Here the term 'bridge' is used to refer to all types of cells that separate solitary vessels, and includes VTs, fibre–tracheids, fibres and axial parenchyma. It is a linear measure of distance between vessels which could act, according to Cai et al. (2014), as a 'hydraulic bridge' in certain species.

Fibre dimensions ($n = 60$ per sample) were manually measured at ×20 magnification in transverse section. Double-fibre wall thickness was measured and the average was divided by 2 to obtain fibre wall thickness. Fibre lumen diameter was measured in two orthogonal axes and their values were averaged. Fibre diameter is the sum of fibre lumen diameter and double-fibre wall thickness.

The percentage of different cell types (fibres, fibre–tracheids, VT and axial parenchyma) was estimated as the amount of each cell type present in macerations, over the total amount of cells ($n \geq 1000$), with images taken at ×20 magnification (15 images per sample). The length of different cell types (fibres, VTs and vessels elements) was also manually estimated in macerations, but at ×4 magnification, 25 vessel elements, 50 fibres and 50 VTs per sample were measured. Rays per lineal millimetre were counted in transverse section (20 images per sample at ×20 magnification) over a perpendicular line to ray orientation. Contact area between vessels and rays was measured manually on images at ×20 magnification in transverse section (20 images per sample). In each vessel whose wall was in contact with rays,

vessel perimeter and contact zone length were measured. This measure was expressed as a percentage, with 100% as the total vessel perimeter.

Conduit wall reinforcement $[(t/b)^2]$ was estimated according to Hacke et al. (2001), where b is the vessel lumen diameter and t is the double vessel wall thickness. Because there are only solitary vessels, and being always in communication with VTs, this parameter was estimated in two ways: (i) considering it as the sum of vessel wall thickness and VT wall thickness $[(t/b)^2]$, and (ii) considering it as the sum of vessel wall thickness and the thickness of the halo surrounding the vessel $[(t/b)^2_h]$. Twenty-five vessel-VT pairs were measured over images in transverse section (×20 magnifications). We hypothesized that the amount of cells surrounding vessels, as well as their wall thickness and turgor level (live cells), could constitute the main wall reinforcement for solitary vessels and contribute to explaining, for example, possible relationships between VC and fibre dimensions or the amount of vasicentric parenchyma.

Wood density was determined in air-dried debarked branches (15% moisture content) as mass/volume. Volume was estimated by fluid displacement.

Additionally, in order to qualitatively confirm that the cellular elements surrounding vessels act as 'bridges' that conduct water, cross-sectional cuts were manually made (freehand) to branch samples where a solution of 0.1% safranin dye was passed through. The dye solution was passed through 30-cm long segments, similar to those used for VC curves, with the pipette method as in k_s determination, with a pressure gradient of 0.007 MPa. We made cuts at different distances from the proximal end of the segment and with different times of dye perfusion (minimum time: when dye just appeared in the distal end of the segment, which took different times depending on the species k_s).

Statistical analyses

The hypotheses were tested by analysing the relationships between pairs of variables with Spearman correlation analysis (since data did not meet normality and homogeneity of variances assumptions). To elucidate VT contribution to xylem function (alternative Hypotheses a and b), we tested the relationship between VT percentage (VT%) and halo area with VC parameters (P_{12}, P_{50}, P_{88}) and $k_{s\ max}$. To determine the trade-off between conduction efficiency and safety (Hypothesis c), we analysed the relationships among VC parameters, $k_{s\ max}$, vessel size and parameters of vessel size distribution curves (b and c PDFV). Hypothesis d was tested by analysing the relationship between reinforcement variables ($(t/b)^2$ and $(t/b)^2_h$) and VC parameters, and Hypothesis e, considering the relationship between wood density and VC parameters, as well as between wood density and anatomical variables describing the fibre matrix and cells surrounding vessels.

In addition to analyses between pairs of variables described before, we performed a multivariate analysis using PCA in order to detect potential associations not considered in our hypotheses. The basic variables were standardized and orthogonal factors (= $F1$, $F2$ and $F3$ axes) were successively built as linear combinations of these variables to maximize the part of the variability explained by these factors.

Significant differences among mean values of variables between species (α = 5%) were detected by non-parametric Kruskal–Wallis H test and were further analysed with a multiple median comparison test (Statistica v.7, Statsoft, Tulsa, OK, USA). Contingency tables were used to establish differences among species in vessel size distribution. We also employed path analysis (InfoStat statistical software v. 2015, InfoStat group, FCA, Universidad Nacional de Córdoba, Córdoba, Argentina) to determine the direct and indirect effects of vessel diameter and halo area over $k_{s\ max}$.

Results

Functional role of cells surrounding vessels (Hypotheses a and b)

Eucalyptus viminalis and *E. camaldulensis* showed similar VC curves, with a clearly sigmoid shape, whereas the *E. globulus* vulnerability curve can be described by an exponential shape (Figure 2). *Eucalyptus globulus* displayed the greatest vulnerability values (P_{50} = −2.44 MPa and P_{12} = −0.61 MPa), which were significantly different from those of the other two species (*E. viminalis*: P_{50} = −3.76 MPa and P_{12} = −1.85 MPa; *E. camaldulensis*: P_{50} = −4.22 MPa and P_{12} = −2.12 MPa). No differences were observed in P_{88} and slope of the curves among the three species (Table 1).

In spite of the differences observed in VC (P_{12} and P_{50}) between *E. globulus* and the other two species, no significant differences were established for VTs among species, either in proportion or in size (Table 1). However, a significant correlation

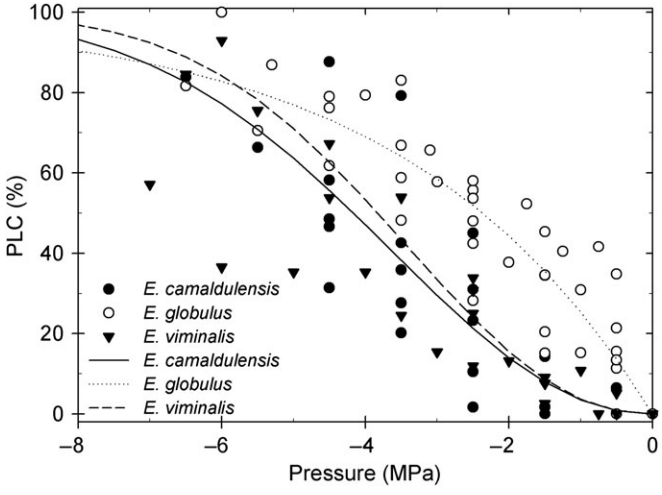

Figure 2. Relationship between PLC and xylem tension (MPa) in four to six branches of *Eucalyptus* spp. Symbols represent PLC at a given pressure for each species branch. Curves represent the predicted PLC by the Weibull model. Parameters and settings of each curve are displayed in Table 1.

Table 1. Mean ± standard deviation of anatomical and functional variables measured in three commercial *Eucalyptus* species ($n = 4–6$) growing in Tandil, Buenos Aires province, Argentina. *H* value from Kruskal–Wallis test and *P* value. Different letters indicate significant differences among species (multiple median comparison tests). Codes for associated probability: ***between 0 and 0.001, **between 0.001 and 0.01, *between 0.01 and 0.05.

	Kruskal–Wallis *H* test	*E. globulus*	*E. viminalis*	*E. camaldulensis*
Vessel diameter (μm)	$H(2,18) = 11.09$**	34.4 ± 6.5 **a**	49.7 ± 3.4 **b**	45.5 ± 4.9 **b**
Vessel number (mm^{-2})	$H(2,18) = 11.68$**	119.7 ± 36.1 **b**	61.5 ± 8.5 **a**	86.8 ± 21.3 **ab**
Halo area (μm^2)	$H(2,18) = 11.82$**	1893.8 ± 343.2 **a**	3168.7 ± 724.4 **b**	2511.5 ± 384.3 **ab**
Halo area/vessel area	$H(2,18) = 1.31$	2.29 ± 0.63	1.87 ± 0.4	1.83 ± 0.3
Conduit wall reinforcement $(t/b)^2$	$H(2,18) = 3.82$	0.012 ± 0.004	0.009 ± 0.004	0.008 ± 0.002
Conduit wall reinforcement (halo) $(t/b)^2_h$	$H(2,18) = 6.89$*	0.23 ± 0.08 **b**	0.14 ± 0.05 **a**	0.14 ± 0.02 **a**
Vessel pit diameter (μm)	$H(2,18) = 13.35$**	5.68 ± 0.63 **b**	4.32 ± 0.33 **a**	6.36 ± 0.45 **b**
VT pit diameter (μm)	$H(2,18) = 5.42$	5.69 ± 0.24	5.47 ± 0.26	5.89 ± 0.30
Bridges (distance) (μm)	$H(2,18) = 0.80$	39.1 ± 9.3	38.8 ± 7.3	37.23 ± 3.2
Bridges (no. of cells)	$H(2,18) = 2.90$	4.66 ± 0.87	4.12 ± 0.85	4.30 ± 0.27
Fibre wall thickness (μm)	$H(2,18) = 5.30$	1.83 ± 0.17	2.07 ± 0.10	1.93 ± 0.23
Fibre diameter (μm)	$H(2,18) = 4.01$	8.56 ± 0.64	8.26 ± 0.62	9.02 ± 0.51
Fibre lumen diameter (μm)	$H(2,18) = 9.58$**	4.90 ± 0.55 **ab**	4.10 ± 0.48 **a**	5.08 ± 0.27 **b**
Fibre percentage (%)	$H(2,18) = 3.10$	80.3 ± 3.8	80.4 ± 4.0	76.8 ± 3.0
Fibre–tracheid percentage (%)	$H(2,18) = 8.08$*	2.92 ± 0.86 **a**	4.22 ± 1.88 **ab**	6.24 ± 1.84 **b**
VT percentage, VT% (%)	$H(2,18) = 1.56$	7.06 ± 1.96	8.82 ± 1.00	8.60 ± 2.08
Axial parenchyma percentage, Ap% (%)	$H(2,18) = 6.22$*	10.43 ± 1.76 **b**	6.57 ± 1.89 **a**	8.33 ± 3.73 **a**
Fibre length (μm)	$H(2,18) = 11.47$**	582.8 ± 19.8 **b**	498.3 ± 15.2 **a**	483.5 ± 45.4 **a**
VT length (μm)	$H(2,18) = 2.00$	365.9 ± 21.9	330.4 ± 28.1	358.3 ± 61.7
Vessel length (μm)	$H(2,18) = 6.98$*	296.7 ± 21.6 **b**	245.2 ± 51.4 **a**	249.8 ± 12.2 **a**
Rays per lineal millimetre (n° mm^{-1})	$H(2,18) = 6.81$*	26.5 ± 5.3 **b**	18.8 ± 3.1 **a**	19.7 ± 2.2 **ab**
Vessel-ray contact (%)	$H(2,18) = 3.35$	36.1 ± 3.5	35.0 ± 3.1	32.5 ± 3.1
Wood density (g cm^{-3})	$H(2,18) = 1.10$	0.771 ± 0.061	0.753 ± 0.052	0.751 ± 0.043
Maximum specific hydraulic conductivity, $k_{s\ max}$ (kg $m^{-1}MPa^{-1}s^{-1}$)	$H(2,15) = 14.36$***	0.32 ± 0.11 **a**	1.79 ± 0.15 **b**	0.95 ± 0.34 **ab**
P_{50} (MPa)	$H(2,15) = 7.24$*	−2.44 ± 0.78 **a**	−3.76 ± 0.44 **ab**	−4.22 ± 0.96 **b**
P_{12} (MPa)	$H(2,15) = 10.49$**	−0.61 ± 0.48 **a**	−1.85 ± 0.52 **ab**	−2.12 ± 0.73 **b**
P_{88} (MPa)	$H(2,15) = 1.40$	−7.48 ± 2.69	−6.07 ± 0.43	−6.79 ± 1.72
Slope of VC curve	$H(2,15) = 2.75$	0.71 ± 0.27	0.93 ± 0.11	0.94 ± 0.37

($\rho = -0.55$, $P < 0.05$) was observed between VT% and P_{12} (see Table S4 available as Supplementary Data at *Tree Physiology* Online), indicating that individuals having more VT proportion are less vulnerable to cavitation at low tension values, thus initiating the exponential phase of cavitation process at lower water potential. In addition, highly significant and negative correlations were observed between P_{12} and P_{50} with halo area around vessels (Figure 3A and B; see Table S4 available as Supplementary Data at *Tree Physiology* Online), which includes VT and parenchyma cells.

Considering the connectivity between VT and vessels, a set of large bordered pits were observed in all radial and tangential walls of VT (Figure 4A). The longest pit chamber axis varied from 5.47 to 5.89 μm (Figure 4B) and species differences were not significant ($P = 0.07$; Table 1). In contrast, vessel pits in *E. viminalis* (mean diameter = 4.32 μm) were significantly smaller (Table 1) than those of *E. globulus* (5.68 μm; Figure 4A and C) and *E. camaldulensis* (6.36 μm). Connection with vessels through pit pairs was detected in transverse section images, sometimes including two pit pairs along tracheid width (arrows in Figure 4D). In agreement with this high connection between vessels and VT, companion cells (VT, fibre–tracheids and axial parenchyma) forming the halo around vessels were rapidly stained when a dye solution was passed through branch segments (Figure 5). The stained area around each vessel increased as dye solution was passed through the segment during more time, and as the distance from the proximal end of the branch segment was shorter. In all cases, some vessels were not stained at all nor their surrounding cells, indicating that the measured branches were partially embolized (Figure 5). No significant differences were found in 'bridge' dimensions among species (Table 1), presenting a length of 37–39 μm and 4–5 cells within this distance, i.e., between two consecutive vessels.

As expected in case of a contribution of cells surrounding vessels to xylem connectivity and efficiency, the halo area (halo area = axial parenchyma + VT) was also high and positively correlated with $k_{s\ max}$ ($\rho = 0.71$, $P < 0.01$; Figure 3C; see Table S4 available as Supplementary Data at *Tree Physiology* Online), and its contribution to $k_{s\ max}$ was significant and complementary to that due to vessel size. However, this last variable was the main contributor in this relationship (according to path analysis).

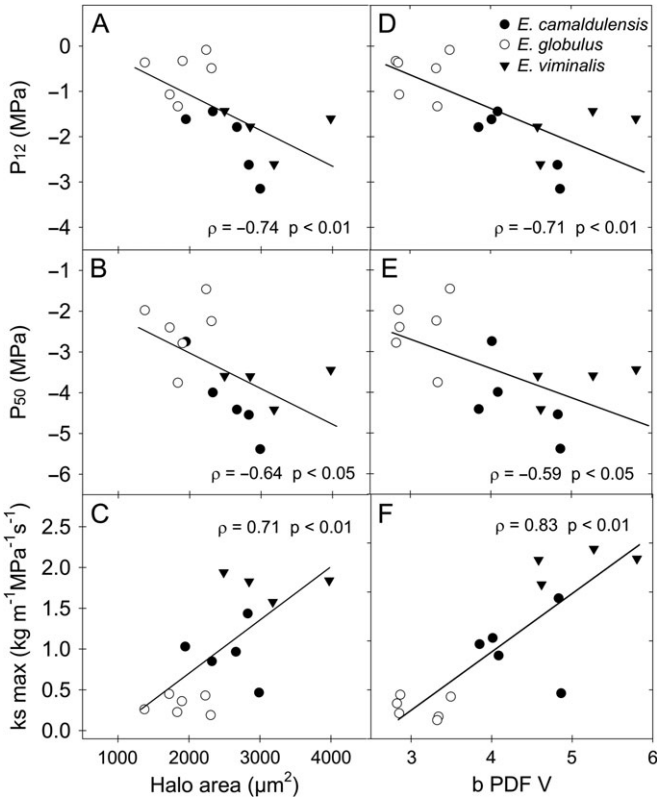

Figure 3. Left column: water potential at 12% of hydraulic conductivity loss (P_{12}; A), water potential at 50% of hydraulic conductivity loss (P_{50}; B) and maximum hydraulic conductivity ($k_{s\ max}$; C) as a function of halo area surrounding vessels. Right column: water potential at 12% of hydraulic conductivity loss (P_{12}; D), water potential at 50% of hydraulic conductivity loss (P_{50}; E) and maximum hydraulic conductivity ($k_{s\ max}$; F) as a function of parameter *b* from Weibull PDF of vessel diameter distribution (which denotes the amplitude of vessel size distribution).

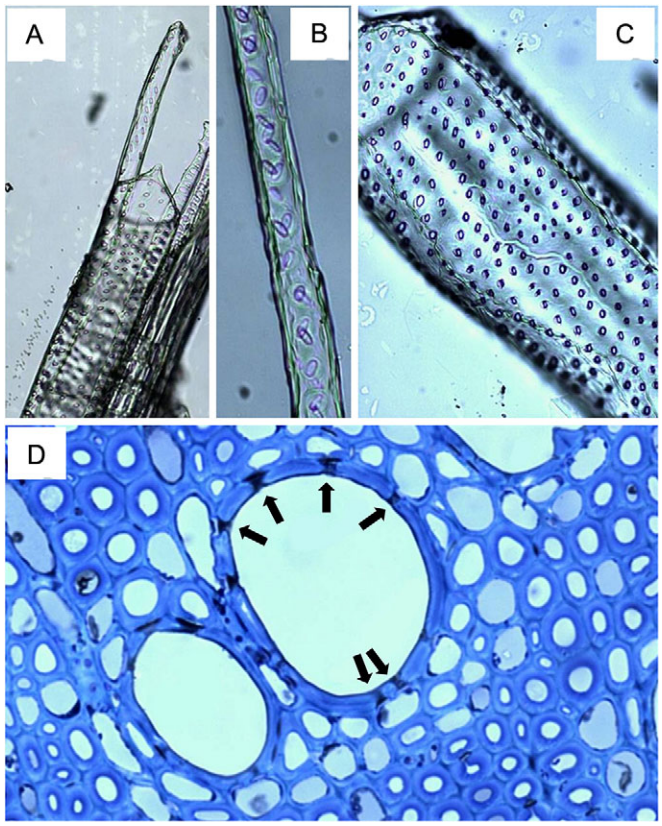

Figure 4. Images of vessel elements (A, C and D) and VTs (A, B and D) on macerations and transverse sections. Detail of VT pits (B) and pit pairs between vessel and VT (D, arrows). Species: *E. globulus*.

It is interesting to note that halo size differed between species, as did its cell composition. *Eucalyptus globulus* presented the smallest halo area but with the highest percentage of axial parenchyma (Table 1).

Trade-off between xylem efficiency and safety (Hypothesis c)

No trade-off was observed between xylem efficiency and safety across the studied *Eucalyptus* species, but the opposite trend: $k_{s\ max}$ was negatively correlated with P_{12} ($\rho = -0.6$, $P < 0.05$; Figure 6B), and marginally related to slope of the VC ($\rho = 0.49$, $P < 0.1$). No significant relationship between $k_{s\ max}$ and the other parameters derived from VC curves (P_{50} and P_{88}) was observed (see Table S4 available as Supplementary Data at *Tree Physiology* Online).

Maximum specific hydraulic conductivity reflected the trends observed in mean vessel diameter ($\rho = 0.8$, $P < 0.01$; see Table S4 available as Supplementary Data at *Tree Physiology* Online) and halo area between them (Figure 3C), with *E. globulus*, the most vulnerable to cavitation species, having the lowest $k_{s\ max}$ (0.32 kg $m^{-1}MPa^{-1}s^{-1}$), followed by *E. camaldulensis* (0.95 kg $m^{-1}MPa^{-1}s^{-1}$) and finally, *E. viminalis* (1.79 kg $m^{-1}MPa^{-1}s^{-1}$). A clear difference is observed in the contribution of each diameter size class for the three species, with *E. viminalis* and *E. camaldulensis* being similar to each other, and significantly different from *E. globulus* ($\chi^2 = 60.08$, $P < 0.01$; Figure 7, left panel). The latter showed a large number of small diameter vessels, which was reflected in its lower average diameter (34 μm). *Eucalyptus viminalis* was at the other end, with small contribution of small vessels (up to 30 μm) with the maximum frequency near its average value (50 μm). The differences in diameter distribution result in diverse curves for cumulative theoretical k_s (estimated by Hagen–Poiseuille law, and relativized to maximum value for each species) as a function of vessel size (Figure 7, right panel). Correlation between measured and theoretical k_s was high ($\rho = 0.8$, $P < 0.01$), but k_s measured experimentally accounted for only 6.41% (*E. globulus*), 10.10% (*E. camaldulensis*) and 14.27% (*E. viminalis*) of $k_{s\ max}$ estimated through vessel diameter distribution. Overall, these curves resemble those of VC, with *E. globulus* showing a steeper slope and a lower mean value on the abscissa than the other two species (see Table S3 available as Supplementary Data at *Tree Physiology* Online). In this regard, we found significant relationships between the parameter *b* of Weibull PDF and P_{12} ($\rho = -0.71$, $P < 0.01$; Figure 3D) and P_{50} ($\rho = -0.59$, $P < 0.05$; Figure 3E).

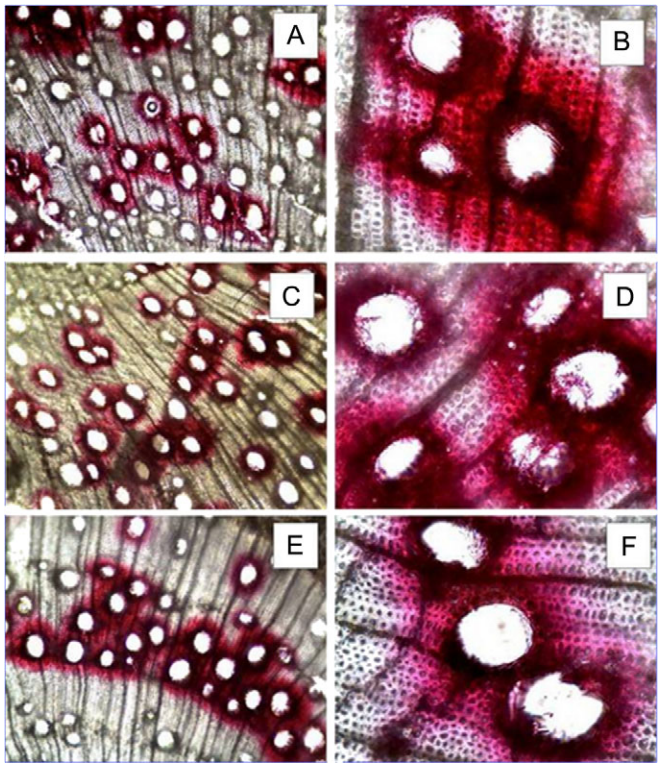

Figure 5. Interconnection among solitary vessels determined by safranin staining. Transverse section images of the three species. A, B: *E. globulus* (×100 and ×400, respectively); C, D: *E. viminalis* (×100 and ×400); E, F: *E. camaldulensis* (×100 and ×400).

This parameter identifies the amplitude of vessel size distribution, indicating that individuals with greater size range were more resistant to cavitation (i.e., they showed more negative values of P_{12} and P_{50}).

Relationship between cell reinforcement and wood density with xylem safety (Hypotheses d and e)

Conduit wall reinforcement $(t/b)^2$ (estimated from walls of connected vessels and VTs; see Materials and methods) showed values between 0.009 and 0.012, with no significant differences between species ($P = 0.15$; Table 1). Instead, $(t/b)^2_h$ (calculated from halo thickness) varied significantly among species ($P = 0.03$), being greater in *E. globulus* (0.23) than in *E. viminalis* and *E. camaldulensis* (0.14). This anatomical parameter showed some marginal ($P < 0.1$) correlation with P_{50} and P_{12} ($\rho = 0.46$ and 0.49, respectively), but in the opposite direction than expected if it acts as mechanical reinforcement: the higher the $(t/b)^2_h$, the greater the cavitation vulnerability.

Unlike what was reported for stem, there were no significant differences in wood density of branches among species ($P = 0.58$; see Table 1). Wood density values ranged between 0.751 and 0.771 g cm^{-3}. Therefore, no relationship was found between wood density and parameters of the VC curve (Spearman correlation test, $P > 0.05$, see Table S4 available as Supplementary Data at *Tree Physiology* Online).

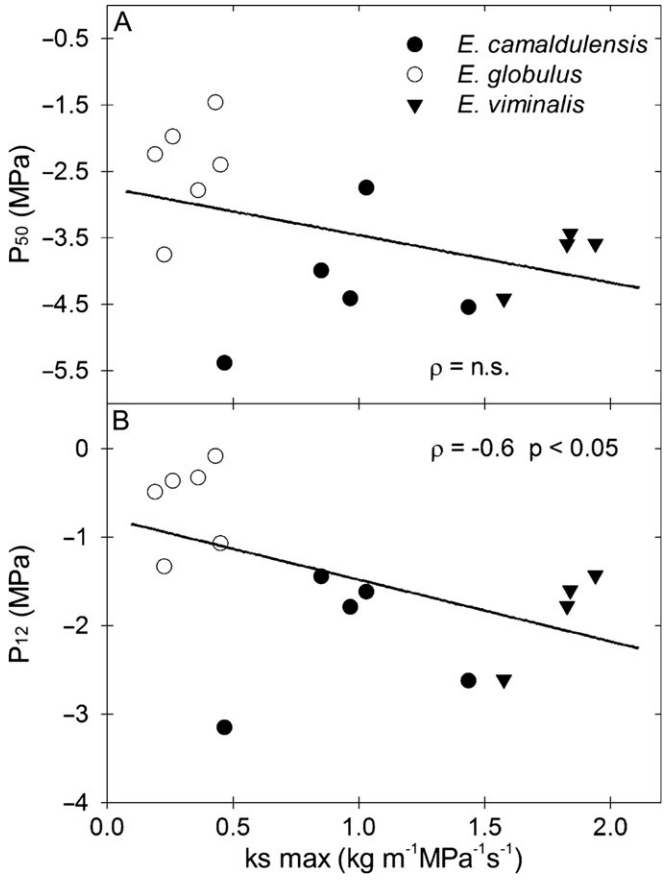

Figure 6. (A) Water potential at 50% of hydraulic conductivity loss (P_{50}) as function of maximum hydraulic conductivity ($k_{s\ max}$) for three *Eucalyptus* species. (B) Water potential at 12% of hydraulic conductivity loss (P_{12}) as a function of $k_{s\ max}$.

Multiple associations between anatomical and functional variables

A general PCA was performed with the individual means of the variables recorded on all trees (Figure 8). Variables are represented on the plane defined by three factorial axes of the PCA, showing the relationship (at the tree level) between wood structure and ecophysiological variables. The first two axes account for 52% of the variation observed between trees (37.9 and 14% for Axes 1 and 2, respectively). Two independent groups of variables were identified in factorial Axes 1 and 2, which allow us to infer the relationship between the structure and function of wood.

Variables associated in Axis 1 were mainly related to water conduction function, including vessels traits (size, number, length—of vessel element—and width of diameter distribution) and traits associated with other cell types: halo area, VTs, rays and conduit wall reinforcement, all of them associated with $k_{s\ max}$ (Figure 8). P_{50} and P_{12} were also associated with Factor 1, but inversely with $k_{s\ max}$.

Factor 2 associated anatomical variables with $k_{s\ max}$ which are difficult to interpret. $k_{s\ max}$ was positively associated with fibre

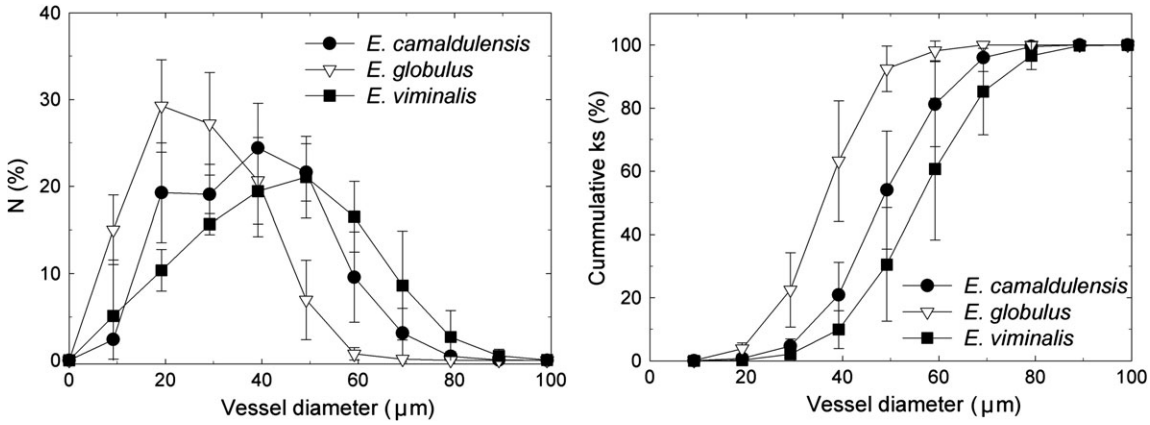

Figure 7. Left panel: vessel-diameter frequency distribution for the three *Eucalyptus* species under study. Right panel: curves of cumulative theoretical k_s (relativized to maximum value for each species) as a function of vessel size. *N* (%), number of vessels in each size class, as a percentage of the total vessel number.

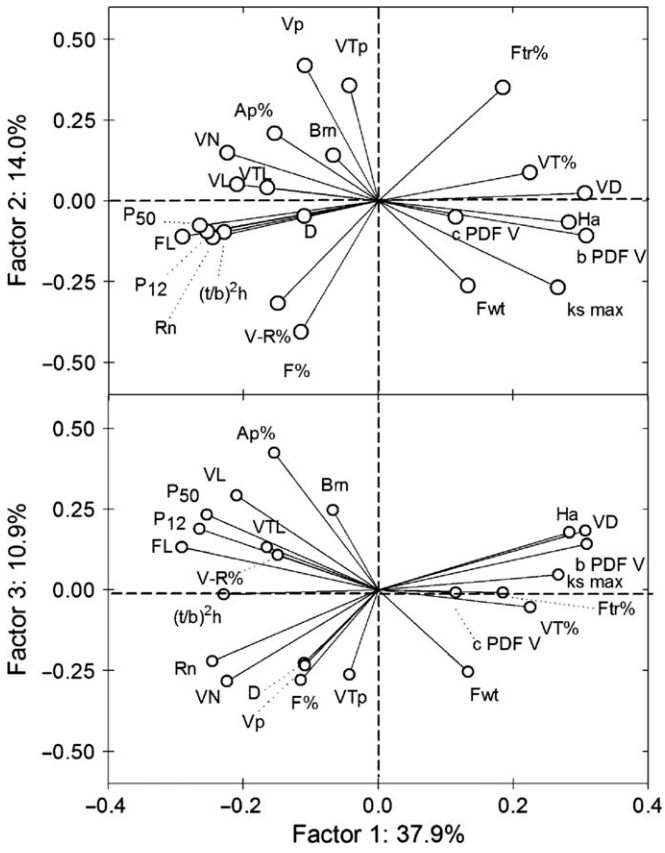

Figure 8. Upper panel: PCA showing Factors 1 and 2. Lower panel: PCA showing Factors 1 and 3. Ap%, axial parenchyma percentage; *b* PDFV, scale parameter of Weibull probability density function; Brn, bridges (no. of cells); *c* PDF V, shape parameter of Weibull probability density function; *D*, wood density, F%, fibre percentage; FL, fibre length; Ftr%, fibre–tracheid percentage; Fwt, fibre wall thickness; Ha, halo area; $k_{s\ max}$, maximum specific hydraulic conductivity; P_{12}, pressure inducing 12% loss of conductivity; P_{50}, pressure inducing 50% loss of conductivity; Rn, rays per lineal millimetre; $(t/b)^2_h$, conduit wall reinforcement; VD, vessel diameter; VL, vessel length; VN, vessel number; Vp, vessel pit diameter; V-R%, vessel–ray contact area; VT%, vasicentric tracheid percentage; VTL, vasicentric tracheid length; VTp, vasicentric tracheid pit diameter; see Table S1 available as Supplementary Data at *Tree Physiology* Online to examine the contribution of each variable.

variables (percentage of fibres and thickness of their walls), and inversely to traits such as pits size and percentage of fibre–tracheids. The third factor, which explained 10.9% of variation, showed an association of variables related to functions of the fibre matrix and parenchyma, such as plant support, carbohydrates storage and embolism repair: percentage of axial parenchyma, number of rays, number of cells between vessels, wood density and fibre wall thickness. P_{50} was also associated with this factor.

Although it is quite difficult to find clear patterns that relate wood anatomy with xylem safety (vulnerability to cavitation) in these *Eucalyptus* species, both P_{50} and P_{12} were well represented along Factor 1, varying inversely with vessel diameter, halo area, the parameter *b* of Weibull PDF (which denotes the amplitude of vessel size distribution), and VT percentage (see Table S5 available as Supplementary Data at *Tree Physiology* Online). These two VC parameters also varied positively with the length of fibres, vessel elements and VTs, conduit wall reinforcement, and ray number (Figure 8), but—as was stated before—in the opposite direction to that expected. In Factor 3, P_{50} (but not P_{12}) was inversely related to wood density and positively to axial parenchyma.

Discussion

In our study, we found s-shaped VC curves in the case of *E. viminalis* and *E. camaldulensis* and r-shaped curves in *E. globulus*. Despite the current debate on methodologies to determine VC in species with long vessels (Christman et al. 2012, Jansen et al. 2015), in this study we found that the species with the longest vessels were those with the highest cavitation resistance (more negative P_{12} and P_{50}), and with s-shaped curves. This is the opposite of what would be expected if there were too many open vessels in branch segments. In addition, P_{50} of *E. camaldulensis* (−4.2 MPa) was very similar to that reported by Trifilò et al.

(2015) for the same species growing in Italy (P_{50} = −4.6 MPa). Moreover, our P_{50} values were below (more cavitation resistant) those reported for other *Eucalyptus* species growing in Australia (Rice et al. 2004), South Africa (Vander Willigen and Pammenter 1998) and Argentina (Tesón et al. 2012). In this regard, we found general evidence in favour of our hypothesis relating mean wood density and VC in *Eucalyptus* species, with species with low wood density, such as *E. grandis* and its hybrid genotypes (mean wood density ~400 kg m^{-3}), being more vulnerable to cavitation (P_{50} ~ −1.5 MPa, determined by both bench dehydration (Vander Willigen and Pammenter 1998) and air injection method (Tesón et al. 2012)). Based on this background, we are confident that our VC curves actually reflect the xylem safety in the studied genotypes. However, further studies comparing VC curves developed with air injection and other methods (like bench dehydration) are needed to validate these results.

Hydraulic role of VTs and parenchyma

Carlquist (1985, 2012) proposed that VTs might have a role in cavitation vulnerability, acting as a subsidiary conducting system when the main system is cavitated. This theory implies that VTs have lower VC than vessels and, at the same time, some conducting capacity that allows the plant to maintain a certain basal water flow. According to this hypothesis, Pratt et al. (2015) pointed out that species with VT of the Californian Chaparral are those with the lower average P_{50}, compared with species with other types of imperforate tracheary elements (fibres, true tracheids and vascular tracheids). However, they noted that it was the group with the highest variance in P_{50} values (including very vulnerable species such as *Quercus berberidifolia*), and therefore the presence of VT per se does not necessarily result in low VC (Pratt et al. 2015). Considering the contribution of VTs to total xylem conductance, although the percentage over total k_s that could be attributed to VTs was not measured here, according to the Hagen–Poiseuille law and the relative size of vessels and VTs, it should be negligible in comparison with k_s developed by vessels, which was partially confirmed by the path analysis performed in our study. Accordingly, Cai et al. (2014), working with *H. rhamnoides* (where they experimentally measured k_s of fibre–tracheids after obstructing vessels artificially), found that it only represents 1.3% of total k_s. In this study, the potential contribution of VTs to increase cavitation resistance in the *Eucalyptus* species under study was partially verified since we found a significant correlation between P_{12} and VT% and halo area, as well as between the latter and P_{50}. In favour of this hypothesis, we observed that these four variables were associated in the same factor of PCA (Factor 1), in an inverse form, which means that individuals with more VT presents lower P_{50} and P_{12}. It is noteworthy that all these species share a common anatomy comprised of large vessels surrounded by VTs, which produces relatively low resistance to water flow and, at the same time, limits the spread of embolisms. This could be achieved by confining embolisms, once they are produced, in companion cells, thus avoiding air dissemination to adjacent vessels.

However, the significant and positive relationship found between $k_{s\ max}$ and halo area suggests that companion cells, VT and/or parenchyma, would also have a function related to conductivity, maybe by increasing connectivity among vessels. In support of this hypothesis, previous modelling and empirical studies in other species have shown an increase in xylem connectivity as a consequence of the presence of imperforate tracheary elements, like VTs (Loepfe et al. 2007, Hacke et al. 2009, Martínez-Vilalta et al. 2012) or hydraulic bridges formed by fibre–tracheids (Cai et al. 2014). Sano et al. (2011) have demonstrated the conductive function of some types of imperforate tracheary elements in a study of 15 angiosperm species (although no *Eucalyptus* species were included) through staining injection, cryo-SEM and other morphometric techniques. According to these authors, size of pits equal or superior to 5 μm and high pit density between vessels and tracheids (77 pits/10,000 μm^2) would suggest, among other things, a conductive role of imperforate elements. In our case, despite the fact that the relationship between $k_{s\ max}$ and halo area was in part due to the correlation between halo area and vessel size, the three species under study exhibited VTs with numerous large pits (5.45–5.89 μm), on both radial and tangential walls. In transverse cuts, pit pairs between vessels and VTs were clearly distinguished (Figure 4D), which would indicate a high contact frequency and, quite possibly, a conductive function of the latter. Likewise, the staining pattern observed in all species (Figure 5) was also consistent with a conductive role—possibly increasing interconnection (Cai et al. 2014)—of the different cell types surrounding vessels.

The functional correlation found in this study between $k_{s\ max}$ and vessel diameter is consistent with the Hagen–Poiseuille law and could be considered as a universal structure–function relationship in plants (Hacke et al. 2009). In addition, we found that *E. viminalis* and *E. camaldulensis*, the species with the longest vessels, were those with the highest $k_{s\ max}$, as is reported for other species (e.g., Lens et al. 2011). In this study, vessel length distribution was not evaluated, but it is expected that this variable could also affect maximum conductivity, particularly in solitary vessel species. However, the highest $k_{s\ max}$ in *E. viminalis* cannot be explained based only on mean vessel size or on pit size (which was the smallest among the studied species). It is clear that other factors, besides the resistance given by vessel walls and the passage through pits, strongly influence the xylem flow capacity in these species with solitary vessels. According to this, our findings on the relationship between halo area and $k_{s\ max}$ could contribute to understanding the role of cells other than vessels in xylem conduction efficiency.

However, according to the relations found in our study, the amount of axial and radial parenchyma does not contribute positively to conductivity (inverse association of rays per linear

millimetre with $k_{s\ max}$ in Factor 1 of PCA and no association of axial parenchyma percentage (Ap%) with $k_{s\ max}$) when making interspecific comparisons. This is because the species with the highest percentage of parenchyma in relation to total tissue (including fibres), such as *E. globulus*, has the lowest $k_{s\ max}$ due to its small vessels and halo areas (in absolute value). Perhaps these relatively small vessels would result in lower k_s, if there were no high connectivity given by the high proportion of bridges and parenchyma tissue. Additionally, there would be an alternative role of these cells (axial and radial parenchyma), more related to embolism repair. These are the only living cells in xylem in contact with solitary vessels that could be involved in the conduction of osmolytes or water for refilling of embolized vessels (Zwieniecki and Holbrook 2009, Brodersen et al. 2010). The positive relationship found among P_{50} and P_{12} with rays (Factors 1 and 3) and Ap% (Factor 3) is in line with this hypothesis, and could be related to a greater capacity to repair embolisms.

Based on these results, it is likely that VTs and parenchyma would contribute to both increasing connectivity between adjacent vessels —and, therefore, to xylem conduction efficiency— and decreasing the probability of embolism propagation into the tissue, i.e., xylem safety.

Role of vessel diameter distribution, fibres and wood density in hydraulic efficiency and safety

It is postulated that, in spite of no causal relationship between vessel size and VC, small vessels are related to greater conductive safety in angiosperm species (e.g., Cai and Tyree 2010). On the contrary, in our study, the most vulnerable to cavitation species, *E. globulus*, presented the smallest vessels. No correlation was observed between $k_{s\ max}$ and VC parameters such as slope, P_{50} and P_{88}. Moreover, we observed a negative correlation between vessel size and $k_{s\ max}$ with P_{12} across all species. This negative correlation implies that individuals with higher $k_{s\ max}$ tended to be less vulnerable to cavitation at low tension values. This result is contrary to evidence reported for many angiosperms species with grouped vessels (Tyree et al. 1994, Pockman and Sperry 2000, Hacke et al. 2001, Lens et al. 2011, Martínez-Vilalta et al. 2012, Gleason et al. 2016) showing a trade-off between efficiency and safety at the xylem level.

Likewise, from the point of view of the physical basis behind the hypothesis developed by Hacke et al. (2001), by which there is a relationship between P_{50} and wood density, it appears to be not applicable for species with the studied type of wood anatomy. This relationship, mediated by a need for reinforcement in vessel walls to avoid xylem implosion that would occur due to contact between embolized and non-embolized vessels, may be not suitable for species with solitary vessels. At best, an embolized vessel would be in contact with tracheids under tension, but surely the pressure differences will distribute differently, since VTs are in contact with a portion of the vessel wall. In accordance with these ideas, the calculation of $(t/b)^2$ resulted in values well below those predicted by Hacke et al. (2001) for the P_{50} values found in our study. Also, no correlation between P_{50} and wood density was found in the studied species. However, some association between reinforcement of the wood matrix around vessels and P_{50} was observed from results of PCA. The third factor positively associated this safety-related trait with wood density and fibre wall thickness. According to this, a study that may be applicable to eucalypts suggests the importance of wood density in cavitation resistance through the contribution of fibre matrix to maintain hydraulic integrity under high tension (Jacobsen et al. 2005).

Conclusions and future research

The (negative) correlation found between hydraulic conductivity and the onset of the cavitation process, added to the lack of relationship with parameters related to later stages, indicates that there is no compromise between efficiency and conductive safety in species with solitary vessels such as *Eucalyptus*. The hydraulic system, composed of large diameter solitary vessels, has relatively high conductive efficiency and may be secure against embolism spread, as was observed in the studied species (but not in all *Eucalyptus* species). It seems that the emergent properties of this complex type of xylem at the 3D level play an important role to overcome trade-offs between efficiency and safety.

The xylem structural strategies of the studied *Eucalyptus* species would result in greater tolerance to high tensions (i.e., at least more tolerant than low wood density *Eucalyptus*, widely grown commercially). An interesting result of this study refers to the relationship found between some parameters describing the VC (P_{12} and P_{50}) and the size distribution of xylem vessels. Individuals with a greater range of vessel size distribution were those which had lower VC. To the best of our knowledge, this kind of pattern has not been previously described, so it deserves a more detailed exploration. Thus, at least in this kind of species with solitary vessels, it seems that a smaller mean vessel size and a narrower vessel size distribution are associated with greater VC at low and medium tension levels.

The specific function of each cell type has not been fully elucidated. Therefore, complementary studies are required, like morphometry and ultrastructure of pits from vessels and tracheids, as well as the development of biophysical hypothesis concerning the operation (embolism spreading among solitary vessels through bridges, role of axial parenchyma in capacitance vs embolism repair) of this type of complex xylem. It is also necessary to complement this work by expanding sample size, adding new sites and genotypes, in order to understand phenotypic plasticity and genetic variability in these characters.

Supplementary Data

Supplementary data for this article are available at *Tree Physiology* Online.

Acknowledgments

The authors wish to thank CONICET (National Council for Scientific and Technical Research of Argentina), AGENCIA (National Agency for Scientific and Technological Promotion) and INTA (National Institute for Agricultural Technology of Argentina) for providing the financial support through PIP0691/2012, PICT2013-1191 and PNFOR1104073, respectively.

Conflict of interest

None declared.

References

Brodersen CR, McElrone AJ, Choat B, Matthews MA, Shackel KA (2010) The dynamics of embolism repair in xylem: in vivo visualizations using high-resolution computed tomography. Plant Physiol 154:1088–1095.

Brodribb TJ, Holbrook NM, Hill RS (2005) Seedling growth in conifers and angiosperms: impacts of contrasting xylem structure. Aust J Bot 53:749–755.

Cai J, Tyree MT (2010) The impact of vessel size on vulnerability curves: data and models for within-species variability in saplings of aspen, *Populus tremuloides* Michx. Plant Cell Environ 33:1059–1069.

Cai J, Li S, Zhang H, Zhang S, Tyree MT (2014) Recalcitrant vulnerability curves: methods of analysis and the concept of fibre bridges for enhanced cavitation resistance. Plant Cell Environ 37:35–44.

Carlquist S (1985) Vasicentric tracheids as a drought survival mechanism in the woody flora of southern California and similar regions: review of vasicentric tracheids. Aliso 11:37–68.

Carlquist S (2012) How wood evolves: a new synthesis. Botany 90:901–940.

Christman MA, Sperry JS, Smith DD (2012) Rare pits, large vessels and extreme vulnerability to cavitation in a ring-porous tree species. New Phytol 193:713–720.

Dadswell HE (1972) The anatomy of eucalypt wood. Forest products laboratory, division of applied chemistry. In: Technical paper No. 66. CSIRO, Melbourne, Australia, p 36.

Domec JC, Gartner BL (2001) Cavitation and water storage capacity in bole xylem segments of mature and young Douglas-fir trees. Trees 15:204–214.

Franklin GL (1945) Preparation of thin sections of synthetic resins and wood-resin composites, and a new macerating method for wood. Nature 155:51.

Gleason SM, Westoby M, Jansen S et al. (2016) Weak tradeoff between xylem safety and xylem-specific hydraulic efficiency across the world's woody plant species. New Phytol 209:123–136.

Greenidge KNH (1952) An approach to the study of vessel length in hardwood species. Am J Bot 39:570–574.

Hacke UG, Sperry JS, Pockman WT, Davis SD, McCulloh KA (2001) Trends in wood density and structure are linked to prevention of xylem implosion by negative pressure. Oecologia 126:457–461.

Hacke UG, Jacobsen AL, Pratt RB (2009) Xylem function of arid-land shrubs from California, USA: an ecological and evolutionary analysis. Plant Cell Environ 32:1324–1333.

Hubbard RM, Ryan MG, Stiller V, Sperry JS (2001) Stomatal conductance and photosynthesis vary linearly with plant hydraulic conductance in Ponderosa pine. Plant Cell Environ 24:113–121.

Iglesias-Trabado G, Wilstermann D (2009) *Eucalyptus* universalis. Global cultivated eucalypt forests map 2009. http://git-forestry-blog.blogspot.com/2008/09/eucalyptus-global-map-2008-cultivated.html (15 October 2015, date last accessed).

InsideWood (2004-onwards) Published on the internet. http://insidewood.lib.ncsu.edu/search (15 October 2015, date last accessed).

Jacobsen AL, Ewers FW, Pratt RB, Paddock WA III, Davis SD (2005) Do xylem fibers affect vessel cavitation resistance? Plant Physiol 139:546–556.

Jansen S, Schuldt B, Choat B (2015) Current controversies and challenges in applying plant hydraulic techniques. New Phytol 205:961–964.

Kondoh S, Yahata H, Nakashizuka T, Kondoh M (2006) Interspecific variation in vessel size, growth and drought tolerance of broad-leaved trees in semi-arid regions of Kenya. Tree Physiol 26:899–904.

Lens F, Sperry JS, Christman MA, Choat B, Rabaey D, Jansen S (2011) Testing hypotheses that link wood anatomy to cavitation resistance and hydraulic conductivity in the genus *Acer*. New Phytol 190:709–723.

Levitt J (ed) (1980) Responses of plants to environmental stresses. Volume II: Water, radiation, salt, and other stresses, 2nd edn. Academic Press, New York.

Loepfe L, Martínez-Vilalta J, Piñol J, Mencuccini M (2007) The relevance of xylem network structure for plant hydraulic efficiency and safety. J Theor Biol 247:788–803.

Maherali H, Pockman WT, Jackson RB (2004) Adaptive variation in the vulnerability of woody plants to xylem cavitation. Ecology 85:2184–2199.

Martínez-Vilalta J, Mencuccini M, Álvarez X, Camacho J, Loepfe L, Piñol J (2012) Spatial distribution and packing of xylem conduits. Am J Bot 99:1189–1196.

Meinzer FC, McCulloh KA (2013) Xylem recovery from drought-induced embolism: where is the hydraulic point of no return? Tree Physiol 33:331–334.

Oliva Carrasco L, Bucci SJ, Di Francescantonio D et al. (2015) Water storage dynamics in the main stem of subtropical tree species differing in wood density, growth rate and life history traits. Tree Physiol 35:354–365.

Pammenter NW, Vander Willigen C (1998) A mathematical and statistical analysis of the curves illustrating vulnerability of xylem to cavitation. Tree Physiol 18:589–593.

Pfautsch S, Renard J, Tjoelker MG, Salih A (2015) Phloem as capacitor: radial transfer of water into xylem of tree stems occurs via symplastic transport in ray parenchyma. Plant Physiol 167:963–971.

Pockman WT, Sperry JS (2000) Vulnerability to xylem cavitation and the distribution of Sonoran desert vegetation. Am J Bot 87:1287–1299.

Pratt RB, Percolla MI, Jacobsen AL (2015) Integrative xylem analysis of chaparral shrubs. In: Hacke U (ed) Functional and ecological xylem anatomy. Springer International Publishing, Switzerland, pp 189–207.

Rice KJ, Matzner SL, Byer W, Brown JR (2004) Patterns of tree dieback in Queensland, Australia: the importance of drought stress and the role of resistance to cavitation. Oecologia 139:190–198.

Sano Y, Morris H, Shimada H, Ronse de Craene LP, Jansen S (2011) Anatomical features associated with water transport in imperforate tracheary elements of vessel-bearing angiosperms. Ann Bot 107:953–964.

Santiago LS, Goldstein G, Meinzer FC, Fisher JB, Machado K, Woodruff D, Jones T (2004) Leaf photosynthetic traits scale with hydraulic conductivity and wood density in Panamanian forest canopy trees. Oecologia 140:543–550.

Scholz FG, Bucci SJ, Goldstein G, Meinzer FC, Franco AC, Miralles-Wilhelm F (2007) Biophysical properties and functional significance of stem water storage tissues in Neotropical savanna trees. Plant Cell Environ 30:236–248.

Sparks JP, Black A (1999) Regulation of water loss in populations of *Populus trichocarpa*: the role of stomatal control in preventing xylem cavitation. Tree Physiol 19:453–459.

Sperry JS, Donnelly JR, Tyree MT (1988) A method for measuring hydraulic conductivity and embolism in xylem. Plant Cell Environ 11:35–40.

Sperry JS, Christman MA, Torrez-Ruiz JM, Taneda H, Smith DD (2012) Vulnerability curves by centrifugation: is there an open vessel artefact,

and are 'r' shaped curves necessarily invalid? Plant Cell Environ 35:601–610.

Tesón N, Fernández ME, Licata J (2012) Resultados preliminares sobre la variación en vulnerabilidad a la cavitación por sequía en clones de *Eucalyptus grandis*. Congreso IUFRO 2012: 'Eucaliptos mejorados para aumentar la competitividad del sector forestal en América Latina'. November 22–23. Pucón, Chile.

Trifilò P, Nardini A, Lo Gullo MA, Barbera PM, Savi T, Raimondo F (2015) Diurnal changes in embolism rate in nine dry forest trees: relationships with species-specific xylem vulnerability, hydraulic strategy and wood traits. Tree Physiol 35:694–705.

Tyree MT, Ewers FW (1991) Tansley Review No. 34. The hydraulic architecture of trees and other woody plants. New Phytol 119:345–360.

Tyree MT, Zimmermann MH (eds) (2002) Xylem structure and the ascent of sap, 2nd edn. Springer, Berlin.

Tyree MT, Davis SD, Cochard H (1994) Biophysical perspectives of xylem evolution: is there a tradeoff of hydraulic efficiency for vulnerability to dysfunction? IAWA J 15:335–360.

Vander Willigen C, Pammenter NW (1998) Relationship between growth and xylem hydraulic characteristics of clones of *Eucalyptus* spp. at contrasting sites. Tree Physiol 18:595–600.

Wheeler JK, Sperry JS, Hacke UG, Hoang N (2005) Inter-vessel pitting and cavitation in woody rosaceae and other vessel led plants: a basis for a safety versus efficiency trade-off in xylem transport. Plant Cell Environ 28:800–812.

Ziemińska K, Butler DW, Gleason SM, Wright IJ, Westoby M (2013) Fibre wall and lumen fractions drive wood density variation across 24 Australian angiosperms. AoB Plants 5:plt046.

Zwieniecki MA, Holbrook NM (2009) Confronting Maxwell's demon: biophysics of xylem embolism repair. Trends Plant Sci 14:530–534.